
Manipulation Intention Understanding for Accurate Zero-Shot Composed Image Retrieval

Anonymous Author(s)

Affiliation

Address

email

Abstract

1 Composed Image Retrieval (CIR) facilitates retrieving an image matching a refer-
2 ence image while incorporating specified textual modifications, which is crucial
3 for internet searches and e-commerce. Traditional supervised CIR methods rely
4 on annotated triplets, which are labor-intensive and limit generalizability. Recent
5 advances in Zero-Shot Composed Image Retrieval (ZS-CIR) address the challenge
6 of performing this task without annotated triplets. A key challenge in ZS-CIR
7 is training models on limited intention-relevant datasets to understand human
8 intention implicitly expressed in textual modifications for accurately retrieving
9 target images. In this paper, we introduce an image-text dataset incorporated
10 with pseudo-manipulation intentions to enhance the training of ZS-CIR models
11 in understanding human manipulation intents. Based on our dataset, we propose
12 a novel framework, De-MINDS, for capturing the intent humans aim to modify,
13 thereby enhancing the ZS-CIR model’s ability to understand human manipulation
14 descriptions. Specifically, a simple mapping network first maps image information
15 into language space and forms a target description with a manipulation descrip-
16 tion. Subsequently, De-MINDS captures intention-relevant information from tar-
17 get descriptions and converts them into several pseudo-word tokens for accurate
18 ZS-CIR. The De-MINDS model exhibits robust generalization and significant
19 improvements in performance across four ZS-CIR tasks. It achieves performance
20 improvements from 2.05% to 4.35% over the best methods and establishes new
21 state-of-the-art results with comparable inference times. Our code is available at
22 <https://anonymous.4open.science/r/De-MINDS/>.

23 1 Introduction

24 Composed Image Retrieval (CIR) [55] aims to retrieve an image that is visually similar to a reference
25 image while having visual modification according to the manipulation text. Different from traditional
26 image retrieval [15], CIR offers more flexibility and accuracy by enabling users to integrate both
27 visual and textual information into their search intent. This approach has gained emerging attention
28 in internet searches and e-commerce applications [12, 45]. Various supervised methods have been
29 proposed to solve CIR problem [12, 33, 19, 4], which requires a large amount of annotated triplets,
30 *i.e.*, a reference image, a manipulated description, and a target image, for training task-specific
31 retrieval models. However, these supervised methods are labor-intensive for data annotation and tend
32 to suffer from limited generalization capabilities due to bias in human annotation. To enhance model
33 generalization and perform CIR tasks without annotated triplets, recent research [45, 3, 52, 25, 20]
34 introduce Zero-Shot Composed Image Retrieval (ZS-CIR). Existing solutions for ZS-CIR map an
35 image to the language space, combining it with text to form a query. This query retrieves target
36 images from the shared semantic space of a pre-trained vision-language model by calculating semantic
37 similarity. These methods typically involve a pre-trained mapping network that converts the reference

38 image into a pseudo-word token S_* . During retrieval, this token S_* is merged with the manipulation
39 description to construct a target description, which a pre-trained CLIP model [41] then encodes,
40 leveraging its comprehensive pre-trained knowledge across image candidates for retrieval.

41 Despite remarkable advancement, the pre-trained mapping networks are not satisfactory for CIR due
42 to the following reasons:

43 (1) There exists a discrepancy between the retrieval and pre-training stages in ZS-CIR models. During
44 retrieval, the mapping network is tasked with aligning intent-specific visual information (*e.g.*, objects,
45 scenes, colors, and styles) in language space to form a composed image description query (*e.g.*,
46 change to a man playing the accordion joyfully in the street) for calculating semantic similarity with
47 the target image. However, in the pre-training phase, the mapping network aligns general visual
48 information with textual descriptions of the image content (*e.g.*, a musician plays the piano). Without
49 intent-specific mapping, the pseudo-token S_* contains heavy information redundancy involving most
50 objects, background/foreground, color, and style, leading to inaccurate retrieval.

51 (2) Accurately understanding the intention a user intends to modify in manipulation descriptions
52 presents substantial challenges. These intentions are implicitly expressed in users’ manipulation
53 descriptions. For instance, the manipulation intention embedded in the request to “make this photo
54 feel like early fall” may involve changing colors (*e.g.*, orange and yellow), adjusting the scene (*e.g.*,
55 fallen leaves), and adding specific objects (*e.g.*, autumnal trees). However, existing ZS-CIR models
56 rely on the CLIP language encoder, which challenges capturing fine-grained/long information from
57 text [51, 58], facing difficulties in accurately understanding these manipulation intentions.

58 In this work, we introduce the intent-CC3M, an intention-based dataset for training mapping net-
59 works capable of aligning intention-relevant visual information within the language space, thus
60 addressing the gap between pre-training and retrieval in ZS-CIR models. We incorporate pseudo-
61 manipulation descriptions in CC3M [47], the widely used ZS-CIR training dataset [45, 52]. These
62 pseudo descriptions, reflecting potential user intention to manipulate images, are reasoned through
63 chain-of-thought prompting using an off-the-shelf Multi-modal Large Language Model (MLLM),
64 facilitating the learning of intent-specific mapping capabilities. Furthermore, to overcome the chal-
65 lenge of existing ZS-CIR models in understanding manipulation intention within descriptions, we
66 propose a novel *unDErstanding of Manipulation INtention from target Description before Searching*
67 approach, named De-MINDS. We leverage pseudo-manipulation descriptions to train De-MINDS
68 to capture manipulation intention from various aspects (*e.g.*, objects, scenes, colors, styles) guided
69 by multiple learnable queries. This intention information is mapped to several pseudo-word tokens,
70 which are subsequently input into the CLIP language encoder, enhancing its ability to understand
71 users’ intention to modify and thereby improving the accuracy of CIR.

72 The main contributions of this work are summarized as follows: (1) We introduce intent-CC3M, a
73 novel dataset with pseudo-manipulation descriptions reasoned by an MLLM to bridge the gap between
74 pre-training and retrieval in ZS-CIR models. Our experiments demonstrate that baseline models
75 trained with our dataset are capable of aligning intention-relevant visual information, achieving
76 consistent performance improvements. (2) We propose a novel manipulation intention understanding
77 network. We extract intentions in manipulation descriptions under the guidance of learnable queries
78 and map to several pseudo-word tokens for retrieval, enhancing the CLIP’s ability to understand users’
79 intentions. It sheds new light on intention-based image retrieval. (3) Our De-MINDS are consistently
80 effective and generalizable across diverse ZS-CIR tasks. It significantly improves CIR performance
81 from 2.05% to 4.35% across four CIR tasks, establishing new state-of-the-art results with comparable
82 inference time, further impacting vision and language applications.

83 2 Related Works

84 **Composed Image Retrieval.** Composed Image Retrieval (CIR) integrates image and text for retrieval
85 [54]. Current models typically employ late fusion for integrating visual and language features
86 separately [4, 33, 4]. In contrast, zero-shot CIR models like Pic2Word [45], SEARLE [3], and
87 Context-I2W [52] train on image-text pairs, bypassing the need for costly CIR datasets. Pic2Word
88 aligns entire images into text features, SEARLE adds a pseudo-word token to GPT-based captions,
89 and Context-I2W employs context-dependent word mapping for accurate retrieval. However, these
90 methods rely on the pre-trained CLIP language encoder, which struggles to understand intentions
91 within manipulation descriptions. To tackle this issue, we propose a novel model that effectively

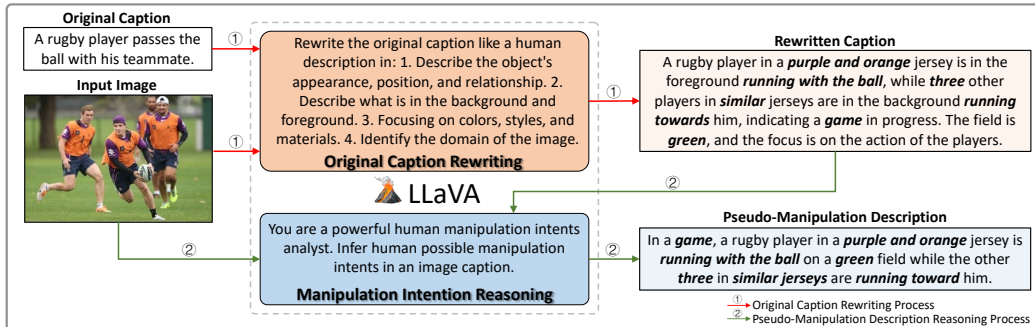


Figure 1: Illustration of using LLaVA to create our intent-CC3M dataset. We first use a prompt to guide the LLaVA model in generating rewritten captions with multi-view visual descriptions. Then, we leverage another prompt to reason pseudo-manipulation descriptions with potential intentions.

92 understands these intentions, thereby improving the ZS-CIR model’s ability to retrieve images based
 93 on human manipulation intents accurately. Unlike CIREVL [25], which employs LLMs during
 94 inference for composed retrieval, introducing non-negligible computational overhead, our model is
 95 lightweight and achieves comparable inference time to recent approaches.

96 **Vision and Language Pre-training Models.** Vision and Language Pre-training (VLP) models, like
 97 CLIP [41], leverage extensive image-text pair training to achieve implicit alignment. Recent VLP
 98 advancements [60, 49] utilize static models to integrate encoded image and text features, enabling
 99 various zero-shot tasks [29, 49, 48]. However, current CLIP-based zero-shot learning struggles with
 100 manipulation description in CIR tasks, motivating our approach, which enhances CLIP’s capabilities
 101 of understanding user intentions to modify from fine-grained/long descriptions. Moreover, recent
 102 studies [1, 28, 38, 37], inspired by DETR [7], employ learnable queries to select image and text
 103 information. In our work, we utilize multiple learnable queries to guide the extraction of manipulation
 104 intentions from target descriptions, providing explanatory cues for more accurate ZS-CIR.

105 **Image-text Dataset Enhancement.** In the field of vision-language learning, various endeavors
 106 [17, 27, 18, 39, 10] aim to enhance caption quality within existing image-text datasets. LaCLIP [17]
 107 utilizes LLMs to refine raw captions. VeCLIP [27] integrates insights from raw and synthetic sources
 108 using LLMs. The latest approach, ShareGPT4V [10], leverages MLLMs to generate descriptive
 109 captions from deliberate prompts and corresponding image inputs. However, these methods ignore
 110 human manipulation intentions, which are crucial for CIR tasks. To bridge this gap, we introduce a
 111 novel dataset infused with pseudo-manipulation intentions reasoned by MLLMs.

112 3 Methodology

113 3.1 Preliminary

114 Given a reference image space \mathcal{I} and a text description space \mathcal{T} , Composed Image Retrieval (CIR)
 115 involves a user manipulation text $T \in \mathcal{T}$ describing hypothetical semantic changes to a reference
 116 image $I_r \in \mathcal{I}$, aiming to retrieve a target image with its closest context from an image database
 117 $\mathcal{D} = \{I_1, \dots, I_n\}$. Zero-Shot CIR (ZS-CIR) approaches [45, 3, 52] sidestep this requirement
 118 by training a mapping network to map the reference image into an associated text representation.
 119 Specifically, these methods learn a mapping function $f_\theta : \mathcal{I} \rightarrow \mathcal{Z}$, where \mathcal{Z} is a pre-defined text-
 120 token embedding space. f_θ is trained using intermediate image representations from a specific image
 121 encoder Ψ_I , often part of a pre-trained vision-language representation system. Template filling
 122 around the manipulation text over the pseudo token embedding $S_* = f_\theta(\Psi_I(I_r))$ is then employed
 123 to aggregate information into a target description P (e.g., “a photo of S_* , $\{T\}$ ”). This target
 124 description serves as input for target image retrieval, encoding it using the associated pre-trained text
 125 encoder Ψ_T . The respective matching score is $\cos_sim(\Psi_I(I_r), \Psi_T(P))$ using cosine similarity.

126 3.2 Creating Intention-based Image-text Alignment Dataset

127 To address the discrepancy between pre-training and retrieval in existing ZS-CIR models, we aim
 128 to develop an intention-based image-text dataset for training mapping networks capable of aligning

129 intent-relevant visual information within the language space. To make a fair comparison and mitigate
 130 the bias in human annotation, we propose to augment the widely used ZS-CIR training image-text
 131 dataset, CC3M, through LLaVA [32], an open-source, state-of-the-art Multi-modal Large Language
 132 Model (MLLM) known for its robust performance in vision-language tasks. However, reasoning
 133 potential manipulation intentions from image-text pairs remains a challenging task for LLaVA.

134 Recent advancements in MLLMs include the development of Chain-of-Thought (CoT) prompting
 135 [56], which enables MLLMs to produce a sequence of reasoning steps, breaking down multi-step
 136 problems into intermediate stages and enhancing performance in complex tasks [24]. Inspired by the
 137 CoT prompting mechanism, we explore a novel multimodal CoT prompting strategy using LLaVA to
 138 reason pseudo-manipulation descriptions with potential intentions from image-text pairs effectively.

139 As illustrated in Figure 1, we divide the process of reasoning pseudo-manipulation descriptions
 140 into two stages: the *Caption Rewriting* stage rewrites the original caption with multi-view visual
 141 information for CIR tasks. The *Intention Reasoning* stage further understands the manipulation
 142 intentions from rewritten captions to reason pseudo-manipulation descriptions. Specifically, in the
 143 caption rewriting stage, we utilize the i -th image I_i and its original caption T_{ori}^i from the CC3M,
 144 denoted as $\mathcal{D} = \{(I_r^i, T_{ori}^i), \dots, (I_r^n, T_{ori}^n)\}$. We guide the LLaVA model with a prompt to generate
 145 a rewritten caption T_{rew}^i for each image. These rewritten captions, averaging 65 tokens, include
 146 various aspects of visual information (e.g., object, foreground/background, color, and domain style).
 147 In the intention reasoning stage, we apply an additional prompt to reason manipulation intention for
 148 rewritten captions. This results in a more effective pseudo-manipulation description T_{int}^i , averaging 27
 149 tokens. The result dataset is represented as $\tilde{\mathcal{D}} = \{(I_r^i, T_{ori}^i, T_{rew}^i, T_{int}^i), \dots, (I_r^n, T_{ori}^n, T_{rew}^n, T_{int}^n)\}$.

150 3.3 Manipulation Intention Understanding From Descriptions Before Searching

151 Since ZS-CIR models leverage the CLIP language encoder, there is a challenge in understanding
 152 manipulation intentions that are implicitly expressed in user descriptions. To address this challenge,
 153 we propose a method to understand the manipulation intention before feeding into the CLIP language
 154 encoder for accurate ZS-CIR in two modules: the *Manipulation Intention Understanding* captures
 155 manipulation intentions and maps them into several pseudo tokens. The *Reasoning Distillation*
 156 further aligns the context of desired pseudo-word tokens closely with human intention by leveraging
 157 pseudo-manipulation description to enhance the models’ ability to understand human intention.

158 **Image and Context Encoding.** For a given sample $(I_r, T_{ori}, T_{rew}, T_{int})$ from intent-CC3M. Since
 159 the pre-trained vision-language models are strong at modeling the cross-modal implicit alignment.
 160 Initially, we employ the frozen image encoder Ψ_I from the CLIP model to encode the global image
 161 feature of the reference image I_r as $\mathbf{v} = \Psi_I(I_r) = \{v_i\}_{i=1}^d \in \mathbb{R}^{d \times 1}$. Subsequently, we apply a
 162 simple mapping network f_θ with parameters θ to extract a pseudo token embedding $S_* = f_\theta(\mathbf{v})$.
 163 Considering our focus on manipulation intention understanding for ZS-CIR, f_θ is structured as a
 164 simple three-layer fully-connected network. We then construct a target description P formatted
 165 as “a photo of S_* , $\{T\}$ ”. We consider two scenarios for manipulation intention understanding:
 166 deducing intention information from concise texts (e.g., original caption) or integrating it from
 167 lengthy texts (e.g., rewritten caption). Accordingly, the text T is composed randomly within a batch
 168 according to the following distribution: 50% original caption T_{rew} and 30% rewritten caption T_{ori} to
 169 learn manipulation intention understanding, 20% pseudo-manipulation description T_{int} to ensure
 170 training stability (details are in Appendix C). We feed the target description to the language encoder
 171 Ψ_T of frozen CLIP to represent the target description P by a set of language feature vectors \mathbf{T}
 172 $= \{\mathbf{t}_i\}_{i=1}^m \subseteq \mathbb{R}^{d \times m}$. \mathbf{t}_1 represents the [CLS] embedding \mathbf{t}_{cls} with global information of image and
 173 caption, while other ones denote word embeddings $\tilde{\mathbf{T}} = \{\mathbf{t}_i\}_{i=2}^m$.

174 **Manipulation Intentions Understanding.** Given the word embeddings of the target descriptions,
 175 this module aims to capture different manipulation intentions, thereby enhancing the CLIP lan-
 176 guage encoder’s capability to understand users’ intents for manipulation. To capture different
 177 manipulation intentions, we introduce a set of learnable query embeddings for guidance, denoted
 178 as $\mathbf{X} = \{\mathbf{x}_k\}_{k=1}^n \in \mathbb{R}^{d \times n}$, where d is the embedding dimension and n is the number of queries.
 179 Each query \mathbf{x}_k represents a kind of manipulation intention. As depicted in Figure 2(left), we im-
 180 plement cross-attention mechanisms to extract intention-relevant contextual information from the
 181 word embeddings $\tilde{\mathbf{T}} = \{\mathbf{t}_i\}_{i=2}^m$ using the learnable queries \mathbf{X} . The cross-attention operation in-
 182 volves three primary steps. First, we compute the query, key and value through linear projections,

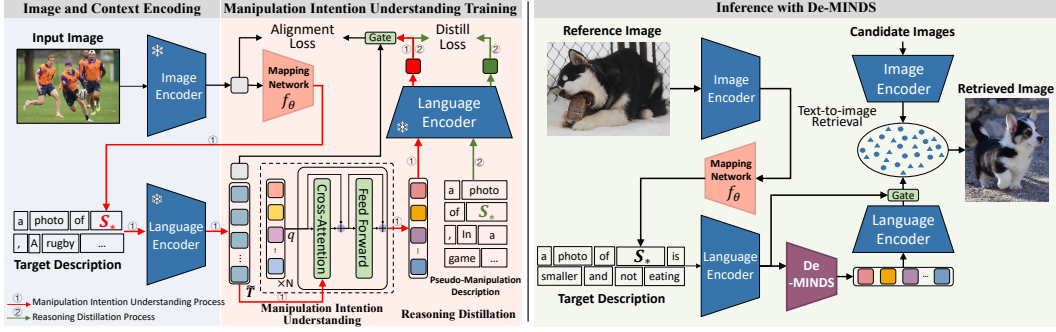


Figure 2: An overview of our De-MINDS. Pre-training (left): Map the image to a pseudo token S_* , and understand the intention from the target description. Inference (right): Map the inference image to S_* to construct the target description and understand manipulation intention for ZS-CIR.

183 *i.e.*, $Q = XW^Q$, $K = [X, \tilde{T}]W^K$, $V = [X, \tilde{T}]W^V$. $[X, \tilde{T}]$ denotes concatenating the two
 184 matrices, which enhances the interaction between learnable queries and word embeddings with better
 185 performance. Then, the learnable queries from the current cross-attention block X^i is calculated as:

$$X_{att}^i = \text{Att}(Q, K, V) = \text{softmax}\left(\frac{QK^\top}{\sqrt{d}}\right)V, X^i = \text{FFW}(X_{att}^i + X^{i-1}) + X_{att}^i \quad (1)$$

186 where X^{i-1} are learnable queries from the previous block and $\text{FFW}(\cdot)$ denotes 2-layer feed-forward
 187 networks. the refined query embeddings X are then fed into the frozen language encoder Ψ_T of
 188 CLIP to extract the intention embedding as $t_* = \Psi_T(X^n) = \{t_*^i\}_{i=1}^d \in \mathbb{R}^{d \times 1}$ ($d = 768$).

189 **Reasoning Distillation.** Given the intention embedding t_* , the AI agent needs to further align with
 190 human manipulation intention. Specifically, we aim to reduce the distance between the intention
 191 embedding and the corresponding pseudo-manipulation description’s [CLS] word embedding, which
 192 represents the MLLM’s intention embedding while ensuring that each embedding remains distinct
 193 and discriminative. Given the intention embeddings $\mathcal{T}_{int} = \{t_*^i\}_{i=1}^N$, where N is the number of
 194 images in \tilde{D} , and the corresponding MLLM’s intention embeddings $\tilde{t}_* = \Psi_T(\mathcal{T}_{int}) \in \tilde{\mathcal{T}}_{int}$ we
 195 employ a symmetric contrastive loss inspired by SimCLR [11, 13, 45] as follows:

$$\mathcal{L}_{distil} = \mathcal{L}_{s2t}(t_*, \tilde{t}_*) + \mathcal{L}_{t2s}(\tilde{t}_*, t_*) \quad (2)$$

196 The two contrastive loss terms are defined as:

$$\mathcal{L}_{s2t}(t_*, \tilde{t}_*) = -\frac{1}{|B|} \sum_{i \in B} \log \frac{e^{\tau(t_*^i)^T \tilde{t}_*^i}}{\sum_{j \in B} e^{\tau(t_*^i)^T \tilde{t}_*^j}}, \mathcal{L}_{t2s}(\tilde{t}_*, t_*) = -\frac{1}{|B|} \sum_{i \in B} \log \frac{e^{\tau(\tilde{t}_*^i)^T t_*^i}}{\sum_{j \in B} e^{\tau(\tilde{t}_*^i)^T t_*^j}} \quad (3)$$

197 where B is the number of images in a batch and τ is a temperature hyper-parameter that controls the
 198 strength of penalties on hard negative samples.

199 **Cross-Modal Alignment.** Given the embedding of user manipulation intention, this module aims
 200 to form a target embedding optimized for retrieval. Since the nature of CIR, both the reference
 201 image and the manipulation intention form a comprehensive context that defines the target image. To
 202 dynamically control the influence of manipulation intentions on the retrieval process, we introduce a
 203 learnable scalar *gate* that decides the contribution of the manipulation intention information t_* and
 204 integrates the global information t_{cls} to form the final target embedding \hat{t} as follows:

$$\hat{t} = t_{cls} + gate \cdot t_*$$

205 Then, we aim to match a target image to its paired target embedding while separating unpaired
 206 ones. We minimize the symmetric contrastive loss between the image embedding v and the target
 207 embedding \hat{t} as follows:

$$\mathcal{L}_{align} = \mathcal{L}_{s2t}(\hat{t}, v) + \mathcal{L}_{t2s}(v, \hat{t}) \quad (4)$$

208 where \mathcal{L}_{s2t} and \mathcal{L}_{t2s} are two contrastive loss terms as Eq.3. The final loss used to optimize is:

$$\mathcal{L} = \mathcal{L}_{distil} + \mathcal{L}_{align} \quad (5)$$

209 **Inference with De-MINDS.** In the inference stage, we compose the reference image with the paired
210 manipulation description and compare the composed query with candidate images for retrieval. As
211 shown in Figure 2 (right), we compose the pseudo token embedding S_* of the image from the
212 mapping network with the text description and feed it to the pre-trained language encoder of CLIP.
213 The result is embedded by the text encoder and compared to the visual features of candidate images.

214 Since we focus on studying the manipulation intention understanding searching for ZS-CIR, we utilize
215 the same prompt in the most recent works [45, 52] for a fair comparison. We show prompt examples
216 for different ZS-CIR tasks. In all examples, [*] indicates the pseudo token from the mapping
217 network: **(a) Domain conversion** aims to modify the domain of the reference image. The prompt
218 is defined as a [domain tag] of [*]; **(b) Object composition** retrieves an image that contains
219 an object in the reference image and other object tags. The prompt is in the format of a photo
220 of [*], [obj₁ tag] and [obj₂ tag], ..., and [obj_n tag]; **(c) Sentence manipulation**
221 modifies the reference image based on a sentence. We simply append the sentence with the special
222 token as a photo of [*], [sentence]. More details are in Appendix D.3.

223 4 Experiments

224 **Datasets.** We evaluate our model on four ZS-CIR datasets, *i.e.*, COCO [31] for object composition,
225 ImageNet [16, 21] for domain conversion, CIRR [33] for object/scene manipulation, and Fashion-IQ
226 [57] for attribute manipulation. All the dataset settings and evaluation metrics (Recall@K) follow the
227 recent works [45, 52] for a fair comparison.

228 (1) Domain conversion. This dataset comprises 16,983 images of 200 classes from four domains,
229 *i.e.*, cartoon, origami, toy, and sculpture. We use the prompt (a) in inference. (2) Object composition.
230 The dataset contains images with corresponding lists of object labels and instance masks of query
231 images. We randomly crop one object and mask its background using its instance mask to create a
232 reference image. We use the prompt (b) in inference. (3) Object/scene manipulation. A reference
233 image is an instruction for manipulating an object or the background scene. We apply the prompt
234 (c) in inference. (4) Attribute manipulation. This dataset includes various description sentences for
235 manipulating image attributes. We utilize the prompt (c) in inference. More details in Appendix D.2.

236 **Implementation Details.** Generating one pseudo-manipulation description through LLaVA-1.6-13B
237 [32] for the entire Conceptual Caption dataset [47], which comprises 3M images (CC3M), requires
238 approximately 625 hours on 5 A100 (80G) GPUs. For training De-MINDS, We utilize the CC3M and
239 adopt ViT-L/14 CLIP [41] pre-trained on 400M image-text paired data. We employ AdamW [34] with
240 a learning rate of 1×10^{-6} , weight decay of 0.1, and a linear warmup of 10000 steps. The number
241 of cross-attention blocks is 6. The number of learnable queries is 4. The batch size for contrastive
242 learning is 1024. To improve training stability, we initialize the learnable scalar of tanh-gating to 0
243 [2]. For training Context-I2W and SEARLE, we keep the same setting reported in their paper, only
244 replacing the original captions with our pseudo-manipulation descriptions. All models are trained on
245 4 NVIDIA A100 (80G) GPUs. To ensure reliable results, we report the performance averaged over
246 three trials. More details are in Appendix D.1.

247 4.1 Quantitative and Qualitative Results

248 We compare De-MINDS with several ZS-CIR methods, including: 1) **Pic2Word** [45]: Maps the
249 visual features of a reference image into a pseudo-word token within the CLIP token embedding
250 space; 2) **SEARLE-XL** [3]: Similar to Pic2Word, further integrating the pseudo-word token with the
251 caption generated by GPT [6] and distilled for efficiency; 3) **Context-I2W** [52]: Selectively extracts
252 text-relevant visual information from the reference image before mapping it into a pseudo-word
253 token; 4) **CIReVL** [25]: Uses LLMs to enhance the manipulation description during inference; and
254 5) **LinCIR** [20]: Masks subjects in captions from various image-text datasets for training. For a fair
255 comparison, we present the reported results of methods relying on the ViT-L/14 CLIP model.

256 Moreover, we compare De-MINDS with 6) **SEARLE-XL* and Context-I2W***: Replace the original
257 captions with our pseudo-manipulation description, and standard ZS-CIR methods, including 7)
258 **Text-only**: Computes similarity based on the CLIP features of descriptions and candidate images; 8)
259 **Image-only**: Retrieves the most similar images to the reference image; and 9) **Image + Text**: Sums
260 the CLIP features of the reference image and the description.

Table 1: Results on Fashion-IQ for attribute manipulation.

Methods	Conferences	Dress		Shrit		TopTee		Average	
		R10	R50	R10	R50	R10	R50	R10	R50
Image-only	–	5.4	13.9	9.9	20.8	8.3	17.7	7.9	17.5
Text-only	–	13.6	29.7	18.9	31.8	19.3	37.0	17.3	32.9
Image+Text	–	16.3	33.6	21.0	34.5	22.2	39.0	19.8	35.7
Pic2Word [45]	CVPR 2023	20.0	40.2	26.2	43.6	27.9	47.4	24.7	43.7
CIReVL [25]	ICLR 2024	24.6	44.8	29.5	47.4	31.4	53.7	28.6	48.6
LinCIR [20]	CVPR 2024	20.9	42.4	29.1	46.8	28.8	50.2	26.3	46.5
SEARLE-XL [3]	ICCV 2023	20.3	43.2	27.4	45.7	29.3	50.2	25.7	46.3
SEARLE-XL*	–	22.7	45.0	29.4	47.9	30.2	51.4	27.4	48.1
Context-I2W [52]	AAAI 2024	23.1	45.3	29.7	48.6	30.6	52.9	27.8	48.9
Context-I2W*	–	23.9	46.9	30.4	49.7	31.1	53.8	28.5	50.1
De-MINDS	–	25.2	48.7	31.0	51.2	32.9	55.7	29.7	51.9

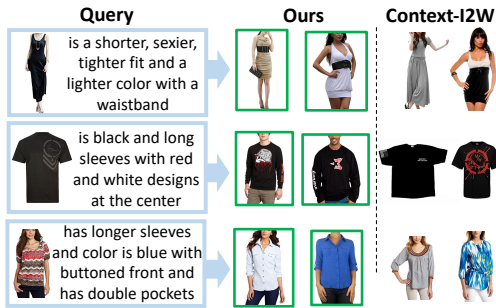


Figure 3: Results on the attribute manipulation task

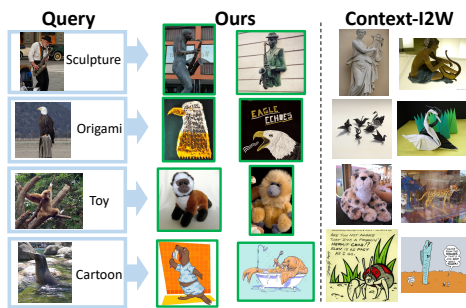


Figure 4: Results on the domain conversion task.

261 Tables 1 to 4 present the quantitative results, while Figures 3 to 6 display the corresponding qualitative
 262 results of our model and the most recent works, CIReVL and Context-I2W. The attribute manipulation
 263 task requires accurately localizing specific attributes within the entire image. As demonstrated in Table
 264 1, De-MINDS outperforms existing ZS-CIR models significantly, achieving an average improvement
 265 of 2.20% over the State-of-the-Art (SoTA) model, CIReVL. CIReVL’s dependency on an LLM at
 266 inference introduces substantial computational overhead during retrieval. De-MINDS tackles this
 267 challenge by extracting fashion-relevant intention within manipulation descriptions into a series of
 268 implicit pseudo-tokens for CLIP retrieval. This approach is more efficient and suitable for models than
 269 relying on explicit, often noisy, LLM analysis results. Figure 3 further illustrates how De-MINDS
 270 effectively understand complex fashion-relevant attributes in manipulation descriptions, such as a
 271 sexier style with a waistband (row 1), black color with a special design in the center (row 2), and
 272 longer sleeves with two pockets in blue (row 3), facilitating more accurate searching.

273 We further assess De-MINDS’ capability in foreground/background differentiation and fine-grained
 274 image editing through the object/scene manipulation task (Table 2). De-MINDS consistently surpasses
 275 existing ZS-CIR models, achieving an average performance improvement of 2.05% over the best
 276 model. This enhancement is attributed to De-MINDS’ approach of extracting human intention from
 277 manipulation descriptions before searching, enhancing the ability of the CLIP language encoder
 278 to understand the user’s intention to modify. In Figure 5, De-MINDS accurately understands
 279 manipulation intention to change the number of an object and modify the background (row 1), alter
 280 the stage and remove an overlapping object (row 2), adjust the camera focus, age of a dog, and
 281 remove a specific object (row 3), and modify the style of an image with a specific design (row 4).

282 In the object composition experiments (Table 3), De-MINDS significantly outperforms the current
 283 SoTA model by an average of 4.30%. These results prove the effectiveness of De-MINDS in
 284 accurately mapping visual information to the language token space via bridges the gap between
 285 pre-training and retrieval, which facilitates the combination of multiple objects, as shown in Figure 6.

286 Moreover, in the domain conversion results (Table 4), De-MINDS consistently outperforms existing
 287 approaches and notably surpasses the SoTA Context-I2W by an average of 4.35%. As illustrated in
 288 Figure 4, De-MINDS accurately maps objects within complex scenes (e.g., a saxophonist in the street,
 289 a bald eagle on wood, a monkey in the forest, and a sea lion in the water). In contrast, Context-I2W
 290 struggles to select the intention-relevant local visual features due to its reliance on image caption
 291 without intention, whereas our pseudo-manipulation descriptions are effectively addressed.

Table 2: Results on CIRR for object manipulation task.

Methods	R1	R5	R10	R50
Image-only	7.4	23.6	34.0	57.4
Text-only	20.9	44.8	55.5	79.1
Image+Text	12.4	36.2	49.1	78.2
Pic2Word [45]	23.9	51.7	65.3	87.8
CIReVL [25]	24.6	52.3	64.9	86.3
LinCIR [20]	25.0	53.3	66.7	–
SEARLE-XL [3]	24.2	52.4	66.3	88.6
SEARLE-XL*	25.4	54.1	66.9	89.3
Context-I2W [52]	25.6	55.1	68.5	89.8
Context-I2W*	26.3	55.7	69.0	90.2
De-MINDS	27.3	57.0	71.3	91.6



Figure 5: Retrieved results on the object manipulation task

Table 3: Results on COCO for object composition task.

Methods	R1	R5	R10
Image-only	8.6	15.4	18.9
Text-only	6.1	15.7	23.5
Image+Text	10.2	20.2	26.6
Pic2Word [45]	11.5	24.8	33.4
Context-I2W [52]	13.5	28.5	38.1
Context-I2W*	14.3	29.7	40.5
De-MINDS	15.7	33.2	44.1

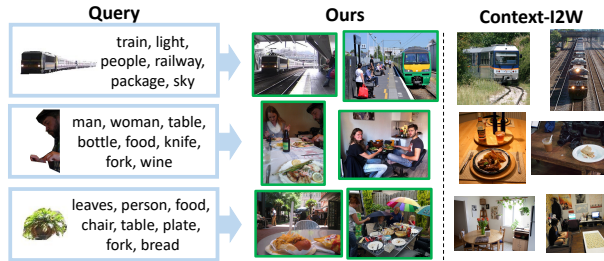


Figure 6: Retrieved results on the object composition task.

Table 4: Results on ImageNet for domain conversion.

Methods	Conferences	Cartoon		Origami		Toy		Sculpture		Average	
		R10	R50	R10	R50	R10	R50	R10	R50	R10	R50
Image-only	–	0.3	4.5	0.2	1.8	0.6	5.7	0.3	4.0	0.4	4.0
Text-only	–	0.2	1.1	0.8	3.7	0.8	2.4	0.4	2.0	0.5	2.3
Image+Text	–	2.2	13.3	2.0	10.3	1.2	9.7	1.6	11.6	1.7	11.2
Pic2Word [45]	CVPR 2023	8.0	21.9	13.5	25.6	8.7	21.6	10.0	23.8	10.1	23.2
Context-I2W [52]	AAAI 2024	10.2	26.1	17.5	28.7	11.6	27.4	12.1	28.2	12.9	27.6
Context-I2W*	–	11.2	27.4	18.7	30.4	12.5	29.8	13.7	31.4	14.0	29.8
De-MINDS	–	13.3	31.2	20.3	34.5	14.7	31.7	16.5	34.7	16.2	33.0

292 4.2 Ablation Study

293 In Table 5, we evaluate the contributions of De-MINDS components on the CIRR and FashionIQ
 294 datasets. (1) **In models ‘2-3’, we assess the significance of the intent-CC3M dataset.** Replacing the
 295 pseudo-manipulation description with original captions (model ‘2’) results in an average performance
 296 drop of 3.80%, demonstrating training with intent-CC3M benefit for aligning intention-relevant
 297 visual information. Using a single prompt for pseudo-manipulation descriptions (model ‘3’) causes a
 298 3.14% performance decline, indicating that CoT prompting enhances MLLM in reasoning potential
 299 manipulation intention. (2) **In models ‘4-6’, we evaluate key modules in the manipulation intention**
 300 **understanding process.** Without intention embeddings from De-MINDS (model ‘4’), performance
 301 drops by 4.02% on average, proving De-MINDS’s importance in CIR. Removing the global feature
 302 t_{cls} (model ‘5’) leads to a 2.38% performance decline, highlighting the necessity of comprehensive
 303 both global and intention information. Summing global and intention features directly (model
 304 ‘6’) causes a 1.64% performance drop, indicating the need for adaptive capture of complementary
 305 information. (3) **In models ‘7-9’, we assess De-MINDS’s training strategies.** Using only original
 306 captions as T (model ‘7’) reduces training stability, resulting in a 1.62% performance drop. Without
 307 the distillation loss (model ‘8’) or replacing it with a cosine loss (model ‘9’) leads to performance
 308 drops of 3.58% and 1.54%, respectively, indicating the necessity of symmetric contrastive loss for
 309 distilling MLLM’s reasoning ability. **In models ‘10-12’, we evaluate alternative solutions.** Not
 310 utilizing T for image-to-text mapping (model ‘10’) results in a 2.30% performance drop, confirming
 311 the effectiveness of our pseudo-manipulation descriptions. Applying MiniGPT-4 [61] to generate the
 312 intent-CC3M dataset (model ‘11’) results in a 1.18% performance drop, suggesting that a superior
 313 MLLM model benefits pseudo-manipulation description quality. Leveraging the LLaMA [53] rewrite

Table 5: Ablation study of main components on CIRR and FashionIQ.

Methods	CIRR			Fashion-IQ	
	R1	R5	R10	R10	R50
1. full model	27.3	57.0	71.3	29.7	51.9
Significant of intent-CC3M					
2. w/o intent-CC3M	24.6	53.7	67.1	26.0	46.8
3. w/o CoT	25.2	54.3	67.8	26.7	47.5
Key modules of De-MINDS process					
4. w/o De-MINDS	24.0	53.5	67.2	25.8	46.6
5. w/o global feature	25.5	55.2	68.0	27.3	49.6
6. w/o gate	25.9	55.3	69.5	27.9	50.4
Training Strategies					
7. w/o construct T	26.2	55.6	69.3	27.8	50.2
8. w/o distil	24.8	53.9	67.3	26.3	47.0
9. cos distill	26.2	55.5	69.7	27.9	50.2
Alternative solutions					
10. a photo of S_*	25.5	55.2	67.9	27.5	49.6
11. MiniGPT4's caption	26.4	55.7	70.2	28.2	50.8
12. LLM's caption	25.2	53.7	67.2	26.9	47.2

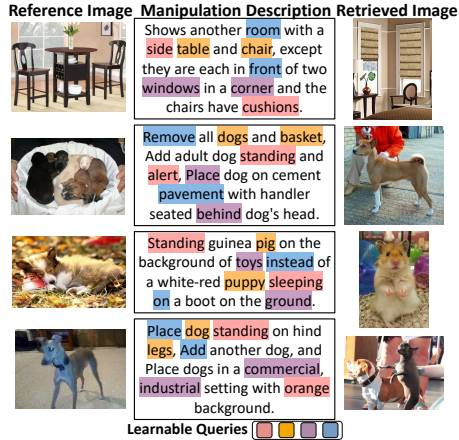


Figure 7: Visualization of the top two attention words for each learnable query, different colors denoting the results corresponding to each query.

314 CC3M dataset [17] (model ‘12’) causes a 3.40% performance drop, indicating the necessity of MLLM
 315 for generating pseudo-manipulation description with multi-view supplementary image detail.

316 4.3 Analysis

317 **Interpretability of Learnable Query.** In Figure 7, we visualize the top two attention words of each
 318 learnable query from the last block, demonstrating the distinct focus of the four queries. Specifically,
 319 the first two queries mainly focus on object and attribute information, while the last two queries
 320 mostly consider foreground/background and relation information. These attention maps substantiate
 321 De-MINDS’s interpretability in extracting specific intention across various descriptions, supporting
 322 the understanding of intention from manipulation descriptions.

323 **Effectiveness and Efficiency Analysis.** Our approach achieves significant improvements on four
 324 widely compared ZR-CIR tasks from 2.05% to 4.35% over the SoTA models. Designed for under-
 325 standing manipulation intention, the model size of De-MINDS(58.5M) is larger than the simple
 326 3-layer MLP mapping (0.9M) of Pic2Word. Consequently, our training time (20 hours) is 6 hours
 327 longer than Pic2Word under the same settings. Notably, our inference time (0.017s) is $\times 58$ faster
 328 than CIReVL (~ 1 s), which uses LLM for inference, and only 0.005s slower than Pic2Word. It’s
 329 worth noting that our model using just 50% of the pre-training data achieves comparable performance
 330 to SoTA models (details are in Appendix A.2).

331 **Limitation.** While the training process for De-MINDS does not introduce significant additional
 332 memory or computational overhead, generating pseudo-manipulation descriptions using MLLMs
 333 can be computationally intensive. Moreover, these pseudo descriptions are not filtered, potentially
 334 introducing irrelevant details that do not align with actual human manipulation intention. Our paper
 335 aims to bridge the gap between pre-training and retrieval in ZS-CIR models and introduce a novel
 336 framework to enhance the model’s capability to understand user intention. Future work could explore
 337 more efficient methods to generate pseudo-manipulation descriptions while maintaining performance.

338 5 Conclusion

339 In this paper, we introduce intent-CC3M, an intention-based dataset featuring pseudo-manipulation
 340 descriptions reasoned through chain-of-thought prompting by an MLLM for training mapping
 341 networks to align intention-relevant visual information. Leveraging intent-CC3M, we propose a
 342 novel manipulation intention understanding network that employs learnable queries to enhance the
 343 models’ capability to understand user intention from manipulation descriptions for accurate CIR.
 344 De-MINDS shows strong generalization ability and remarkably improves the best performance of
 345 existing approaches on four diverse ZS-CIR tasks with comparable inference times. Our work inspires
 346 intention-based image retrieval and impacts diverse vision and language applications.

References

- [1] Jean-Baptiste Alayrac, Jeff Donahue, Pauline Luc, Antoine Miech, Iain Barr, Yana Hasson, Karel Lenc, Arthur Mensch, Katherine Millican, Malcolm Reynolds, Roman Ring, Eliza Rutherford, Serkan Cabi, Tengda Han, Zhitao Gong, Sina Samangooei, Marianne Monteiro, Jacob L Menick, Sebastian Borgeaud, Andy Brock, Aida Nematzadeh, Sahand Sharifzadeh, Mikołaj Bińkowski, Ricardo Barreira, Oriol Vinyals, Andrew Zisserman, and Karén Simonyan. Flamingo: a visual language model for few-shot learning. In S. Koyejo, S. Mohamed, A. Agarwal, D. Belgrave, K. Cho, and A. Oh, editors, *Advances in Neural Information Processing Systems*, volume 35, pages 23716–23736, 2022.
- [2] Thomas Bachlechner, Bodhisattwa Prasad Majumder, Henry Mao, Gary Cottrell, and Julian McAuley. Rezero is all you need: Fast convergence at large depth. In *Uncertainty in Artificial Intelligence*, pages 1352–1361, 2021.
- [3] Alberto Baldrati, Lorenzo Agnolucci, Marco Bertini, and Alberto Del Bimbo. Zero-shot composed image retrieval with textual inversion. *arXiv:2303.15247*, 2023.
- [4] Alberto Baldrati, Marco Bertini, Tiberio Uricchio, and Alberto Del Bimbo. Effective conditioned and composed image retrieval combining clip-based features. In *Proceedings of the IEEE/CVF Conference on Computer Vision and Pattern Recognition*, pages 21466–21474, June 2022.
- [5] Lucas Beyer, Xiaohua Zhai, Amélie Royer, Larisa Markeeva, Rohan Anil, and Alexander Kolesnikov. Knowledge distillation: A good teacher is patient and consistent. In *Proceedings of the IEEE/CVF conference on computer vision and pattern recognition*, pages 10925–10934, 2022.
- [6] Tom Brown, Benjamin Mann, Nick Ryder, Melanie Subbiah, Jared D Kaplan, Prafulla Dhariwal, Arvind Neelakantan, Pranav Shyam, Girish Sastry, Amanda Askell, Sandhini Agarwal, Ariel Herbert-Voss, Gretchen Krueger, Tom Henighan, Rewon Child, Aditya Ramesh, Daniel Ziegler, Jeffrey Wu, Clemens Winter, Chris Hesse, Mark Chen, Eric Sigler, Mateusz Litwin, Scott Gray, Benjamin Chess, Jack Clark, Christopher Berner, Sam McCandlish, Alec Radford, Ilya Sutskever, and Dario Amodei. Language models are few-shot learners. In H. Larochelle, M. Ranzato, R. Hadsell, M.F. Balcan, and H. Lin, editors, *Advances in Neural Information Processing Systems*, volume 33, pages 1877–1901. Curran Associates, Inc., 2020.
- [7] Nicolas Carion, Francisco Massa, Gabriel Synnaeve, Nicolas Usunier, Alexander Kirillov, and Sergey Zagoruyko. End-to-end object detection with transformers. In *European conference on computer vision*, pages 213–229, 2020.
- [8] Akshay Chawla, Hongxu Yin, Pavlo Molchanov, and Jose Alvarez. Data-free knowledge distillation for object detection. In *Proceedings of the IEEE/CVF Winter Conference on Applications of Computer Vision*, pages 3289–3298, 2021.
- [9] Guobin Chen, Wongun Choi, Xiang Yu, Tony Han, and Manmohan Chandraker. Learning efficient object detection models with knowledge distillation. In *Proc. of Advances in Neural Information Processing Systems (NeurIPS)*, volume 30, 2017.
- [10] Lin Chen, Jisong Li, Xiaoyi Dong, Pan Zhang, Conghui He, Jiaqi Wang, Feng Zhao, and Dahua Lin. Sharegpt4v: Improving large multi-modal models with better captions. *arXiv preprint arXiv:2311.12793*, 2023.
- [11] Ting Chen, Simon Kornblith, Mohammad Norouzi, and Geoffrey Hinton. A simple framework for contrastive learning of visual representations. In *Proc. of International Conference on Machine Learning (ICML)*, pages 1597–1607. PMLR, 2020.
- [12] Yanbei Chen, Shaogang Gong, and Loris Bazzani. Image search with text feedback by visiolinguistic attention learning. In *Proceedings of the IEEE/CVF Conference on Computer Vision and Pattern Recognition*, pages 3001–3011, 2020.
- [13] Niv Cohen, Rinon Gal, Eli A. Meir, Gal Chechik, and Yuval Atzmon. "This is my unicorn, Fluffy": Personalizing frozen vision-language representations. In *Proc. of the European Conference on Computer Vision (ECCV)*, 2022.
- [14] Niv Cohen, Rinon Gal, Eli A. Meir, Gal Chechik, and Yuval Atzmon. "this is my unicorn, fluffy": Personalizing frozen vision-language representations. In *European conference on computer vision*, pages 558–577, 2022.
- [15] Ritendra Datta, Dhiraj Joshi, Jia Li, and James Z Wang. Image retrieval: Ideas, influences, and trends of the new age. *ACM Computing Surveys*, 40(2):1–60, 2008.
- [16] Jia Deng, Wei Dong, Richard Socher, Li-Jia Li, Kai Li, and Li Fei-Fei. Imagenet: A large-scale hierarchical image database. In *Computer Vision and Pattern Recognition*, pages 248–255, 2009.
- [17] Lijie Fan, Dilip Krishnan, Phillip Isola, Dina Katabi, and Yonglong Tian. Improving clip training with language rewrites. *Advances in Neural Information Processing Systems*, 36, 2024.
- [18] Samir Yitzhak Gadre, Gabriel Ilharco, Alex Fang, Jonathan Hayase, Georgios Smyrnis, Thao Nguyen, Ryan Marten, Mitchell Wortsman, Dhruva Ghosh, Jieyu Zhang, et al. Datacomp: In search of the next generation of multimodal datasets. *Advances in Neural Information Processing Systems*, 36, 2024.
- [19] Sonam Goenka, Zhaoheng Zheng, Ayush Jaiswal, Rakesh Chada, Yue Wu, Varsha Hedau, and Pradeep Natarajan. Fashionvlp: Vision language transformer for fashion retrieval with feedback. In *Proceedings of the IEEE/CVF Conference on Computer Vision and Pattern Recognition*, pages 14105–14115, June 2022.

- 409 [20] Geonmo Gu, Sanghyuk Chun, Wonjae Kim, , Yooheon Kang, and Sangdoon Yun. Language-only efficient
410 training of zero-shot composed image retrieval. In *Conference on Computer Vision and Pattern Recognition*
411 (*CVPR*), 2024.
- 412 [21] Dan Hendrycks, Steven Basart, Norman Mu, Saurav Kadavath, Frank Wang, Evan Dorundo, Rahul Desai,
413 Tyler Zhu, Samyak Parajuli, Mike Guo, Dawn Song, Jacob Steinhardt, and Justin Gilmer. The many faces
414 of robustness: A critical analysis of out-of-distribution generalization. In *Proceedings of the IEEE/CVF*
415 *International Conference on Computer Vision*, pages 8340–8349, 2021.
- 416 [22] Geoffrey Hinton, Oriol Vinyals, and Jeffrey Dean. Distilling the knowledge in a neural network. In *NIPS*
417 *Deep Learning and Representation Learning Workshop*, 2015.
- 418 [23] Sepp Hochreiter and Jürgen Schmidhuber. Long short-term memory. *Neural computation*, 9(8):1735–1780,
419 1997.
- 420 [24] Shaohan Huang, Li Dong, Wenhui Wang, Yaru Hao, Saksham Singhal, Shuming Ma, Tengchao Lv, Lei
421 Cui, Owais Khan Mohammed, Barun Patra, et al. Language is not all you need: Aligning perception with
422 language models. *Advances in Neural Information Processing Systems*, 36, 2024.
- 423 [25] Shyamgopal Karthik, Karsten Roth, Massimiliano Mancini, and Zeynep Akata. Vision-by-language
424 for training-free compositional image retrieval. In *The Twelfth International Conference on Learning*
425 *Representations*, 2024.
- 426 [26] Nupur Kumari, Bingliang Zhang, Richard Zhang, Eli Shechtman, and Jun-Yan Zhu. Multi-concept
427 customization of text-to-image diffusion. In *Proceedings of the IEEE/CVF Conference on Computer Vision*
428 *and Pattern Recognition*, pages 1931–1941, 2023.
- 429 [27] Zhengfeng Lai, Haotian Zhang, Wentao Wu, Haoping Bai, Aleksei Timofeev, Xianzhi Du, Zhe Gan,
430 Jiulong Shan, Chen-Nee Chuah, Yinfei Yang, et al. From scarcity to efficiency: Improving clip training via
431 visual-enriched captions. *arXiv preprint arXiv:2310.07699*, 2023.
- 432 [28] Junnan Li, Dongxu Li, Silvio Savarese, and Steven Hoi. Blip-2: Bootstrapping language-image pre-training
433 with frozen image encoders and large language models, 2023.
- 434 [29] Junnan Li, Dongxu Li, Caiming Xiong, and Steven Hoi. BLIP: Bootstrapping language-image pre-training
435 for unified vision-language understanding and generation. In *Proceedings of the 39th International*
436 *Conference on Machine Learning*, pages 12888–12900, 2022.
- 437 [30] Xiujun Li, Xi Yin, Chunyuan Li, Pengchuan Zhang, Xiaowei Hu, Lei Zhang, Lijuan Wang, Houdong
438 Hu, Li Dong, Furu Wei, et al. Oscar: Object-semantics aligned pre-training for vision-language tasks. In
439 *European Conference on Computer Vision*, pages 121–137, 2020.
- 440 [31] Tsung-Yi Lin, Michael Maire, Serge Belongie, James Hays, Pietro Perona, Deva Ramanan, Piotr Dollár,
441 and C. Lawrence Zitnick. Microsoft coco: Common objects in context. In David Fleet, Tomas Pajdla,
442 Bernt Schiele, and Tinne Tuytelaars, editors, *European Conference on Computer Vision*, pages 740–755,
443 2014.
- 444 [32] Haotian Liu, Chunyuan Li, Qingyang Wu, and Yong Jae Lee. Visual instruction tuning. *Advances in neural*
445 *information processing systems*, 36, 2024.
- 446 [33] Zheyuan Liu, Cristian Rodriguez-Opazo, Damien Teney, and Stephen Gould. Image retrieval on real-life
447 images with pre-trained vision-and-language models. In *Proceedings of the IEEE/CVF International*
448 *Conference on Computer Vision*, pages 2125–2134, October 2021.
- 449 [34] Ilya Loshchilov and Frank Hutter. Decoupled weight decay regularization. In *International Conference on*
450 *Learning Representations*, 2018.
- 451 [35] Chenlin Meng, Robin Rombach, Ruiqi Gao, Diederik Kingma, Stefano Ermon, Jonathan Ho, and Tim
452 Salimans. On distillation of guided diffusion models. In *Proceedings of the IEEE/CVF Conference on*
453 *Computer Vision and Pattern Recognition*, pages 14297–14306, 2023.
- 454 [36] Ron Mokady, Amir Hertz, and Amit H. Bermano. Clipcap: Clip prefix for image captioning, 2021.
- 455 [37] Muhammad Ferjad Naeem, Muhammad Gul Zain Ali Khan, Yongqin Xian, Muhammad Zeshan Afzal,
456 Didier Stricker, Luc Van Gool, and Federico Tombari. I2mvformer: Large language model generated
457 multi-view document supervision for zero-shot image classification. In *Proceedings of the IEEE/CVF*
458 *Conference on Computer Vision and Pattern Recognition*, pages 15169–15179, 2023.
- 459 [38] Muhammad Ferjad Naeem, Yongqin Xian, Luc V Gool, and Federico Tombari. I2dformer: Learning image
460 to document attention for zero-shot image classification. *Advances in Neural Information Processing*
461 *Systems*, 35:12283–12294, 2022.
- 462 [39] Thao Nguyen, Samir Yitzhak Gadre, Gabriel Ilharco, Sewoong Oh, and Ludwig Schmidt. Improving
463 multimodal datasets with image captioning. *Advances in Neural Information Processing Systems*, 36, 2024.
- 464 [40] Adam Paszke, Sam Gross, Francisco Massa, Adam Lerer, James Bradbury, Gregory Chanan, Trevor Killeen,
465 Zeming Lin, Natalia Gimelshein, Luca Antiga, et al. Pytorch: An imperative style, high-performance deep
466 learning library. *NeurIPS*, 32, 2019.
- 467 [41] Alec Radford, Jong Wook Kim, Chris Hallacy, Aditya Ramesh, Gabriel Goh, Sandhini Agarwal, Girish
468 Sastry, Amanda Askell, Pamela Mishkin, Jack Clark, Gretchen Krueger, and Ilya Sutskever. Learning trans-
469 ferable visual models from natural language supervision. In *Proceedings of the International Conference*
470 *on Machine Learning*, pages 8748–8763, 2021.
- 471 [42] Aditya Ramesh, Mukul Goyal, and Rob Fergus. Dall-e: Creating images from text. OpenAI Blog, 2021.

- 472 [43] Adriana Romero, Nicolas Ballas, Samira Ebrahimi Kahou, Antoine Chassang, Carlo Gatta, and Yoshua
473 Bengio. FitNets: Hints for thin deep nets. *arXiv preprint arXiv:1412.6550*, 2014.
- 474 [44] Nataniel Ruiz, Yuanzhen Li, Varun Jampani, Yael Pritch, Michael Rubinstein, and Kfir Aberman. Dream-
475 booth: Fine tuning text-to-image diffusion models for subject-driven generation. In *Proceedings of the*
476 *IEEE/CVF Conference on Computer Vision and Pattern Recognition*, pages 22500–22510, 2023.
- 477 [45] Kuniaki Saito, Kihyuk Sohn, Xiang Zhang, Chun-Liang Li, Chen-Yu Lee, Kate Saenko, and Tomas Pfister.
478 Pic2word: Mapping pictures to words for zero-shot composed image retrieval. In *Proceedings of the*
479 *IEEE/CVF Conference on Computer Vision and Pattern Recognition*, pages 19305–19314, 2023.
- 480 [46] Axel Sauer, Dominik Lorenz, Andreas Blattmann, and Robin Rombach. Adversarial diffusion distillation.
481 *arXiv preprint arXiv:2311.17042*, 2023.
- 482 [47] Piyush Sharma, Nan Ding, Sebastian Goodman, and Radu Soricut. Conceptual captions: A cleaned,
483 hypemymed, image alt-text dataset for automatic image captioning. In *Annual Meeting of the Association*
484 *for Computational Linguistics*, pages 2556–2565, 2018.
- 485 [48] Jiangming Shi, Yachao Zhang, Xiangbo Yin, Yuan Xie, Zhizhong Zhang, Jianping Fan, Zhongchao Shi,
486 and Yanyun Qu. Dual pseudo-labels interactive self-training for semi-supervised visible-infrared person
487 re-identification. In *Proceedings of the IEEE/CVF International Conference on Computer Vision*, pages
488 11218–11228, 2023.
- 489 [49] Haoyu Song, Li Dong, Wei-Nan Zhang, Ting Liu, and Furu Wei. Clip models are few-shot learners:
490 Empirical studies on vqa and visual entailment, 2022.
- 491 [50] Derek Tam, Colin Raffel, and Mohit Bansal. Simple weakly-supervised image captioning via CLIP’s
492 multimodal embeddings. In *The AAAI-23 Workshop on Creative AI Across Modalities*, 2023.
- 493 [51] Yingtian Tang, Yutaro Yamada, Yoyo Zhang, and Ilker Yildirim. When are lemons purple? the concept
494 association bias of vision-language models. In *Proceedings of the 2023 Conference on Empirical Methods*
495 *in Natural Language Processing*, pages 14333–14348, 2023.
- 496 [52] Yuanmin Tang, Jing Yu, Keke Gai, Jiamin Zhuang, Gang Xiong, Yue Hu, and Qi Wu. Context-i2w: Map-
497 ping images to context-dependent words for accurate zero-shot composed image retrieval. In *Proceedings*
498 *of the AAAI Conference on Artificial Intelligence*, volume 38, pages 5180–5188, 2024.
- 499 [53] Hugo Touvron, Thibaut Lavril, Gautier Izacard, Xavier Martinet, Marie-Anne Lachaux, Timothée Lacroix,
500 Baptiste Rozière, Naman Goyal, Eric Hambro, Faisal Azhar, et al. Llama: Open and efficient foundation
501 language models. *arXiv preprint arXiv:2302.13971*, 2023.
- 502 [54] Nam Vo, Lu Jiang, Chen Sun, Kevin Murphy, Li-Jia Li, Li Fei-Fei, and James Hays. Composing text
503 and image for image retrieval - an empirical odyssey. In *Proceedings of the IEEE/CVF Conference on*
504 *Computer Vision and Pattern Recognition*, pages 6439–6448, 2019.
- 505 [55] Nam Vo, Lu Jiang, Chen Sun, Kevin Murphy, Li-Jia Li, Li Fei-Fei, and James Hays. Composing text and
506 image for image retrieval-an empirical odyssey. In *Proceedings of the IEEE/CVF conference on computer*
507 *vision and pattern recognition*, pages 6439–6448, 2019.
- 508 [56] Jason Wei, Xuezhi Wang, Dale Schuurmans, Maarten Bosma, Fei Xia, Ed Chi, Quoc V Le, Denny
509 Zhou, et al. Chain-of-thought prompting elicits reasoning in large language models. *Advances in neural*
510 *information processing systems*, 35:24824–24837, 2022.
- 511 [57] Hui Wu, Yupeng Gao, Xiaoxiao Guo, Ziad Al-Halah, Steven Rennie, Kristen Grauman, and Rogerio Feris.
512 Fashion iq: A new dataset towards retrieving images by natural language feedback. In *Proceedings of the*
513 *IEEE/CVF Conference on Computer Vision and Pattern Recognition*, pages 11307–11317, 2021.
- 514 [58] Beichen Zhang, Pan Zhang, Xiaoyi Dong, Yuhang Zang, and Jiaqi Wang. Long-clip: Unlocking the
515 long-text capability of clip, 2024.
- 516 [59] Pengchuan Zhang, Xiujun Li, Xiaowei Hu, Jianwei Yang, Lei Zhang, Lijuan Wang, Yejin Choi, and
517 Jianfeng Gao. Vinvl: Revisiting visual representations in vision-language models. In *Proceedings of the*
518 *IEEE/CVF Conference on Computer Vision and Pattern Recognition*, pages 5579–5588, 2021.
- 519 [60] Kaiyang Zhou, Jingkang Yang, Chen Change Loy, and Ziwei Liu. Conditional prompt learning for
520 vision-language models. In *Proceedings of the IEEE/CVF Conference on Computer Vision and Pattern*
521 *Recognition*, pages 16816–16825, 2022.
- 522 [61] Deyao Zhu, Jun Chen, Xiaoqian Shen, Xiang Li, and Mohamed Elhoseiny. Minigt-4: Enhancing
523 vision-language understanding with advanced large language models. *arXiv preprint arXiv:2304.10592*,
524 2023.
- 525 [62] Wanrong Zhu, An Yan, Yujie Lu, Wenda Xu, Xin Eric Wang, Miguel Eckstein, and William Yang Wang.
526 Visualize before you write: Imagination-guided open-ended text generation, 2023.

527 A Extended Analysis

528 A.1 Analysis of the number of learnable queries.

529 We conduct analysis on the number of learnable query embedding $\mathbf{X} = \{\mathbf{x}_k\}_{k=1}^n \in \mathbb{R}^{d \times n}$ as shown
530 in Figure 8. We find that $n = 2$ results in not learning sufficient intentions for manipulation, but

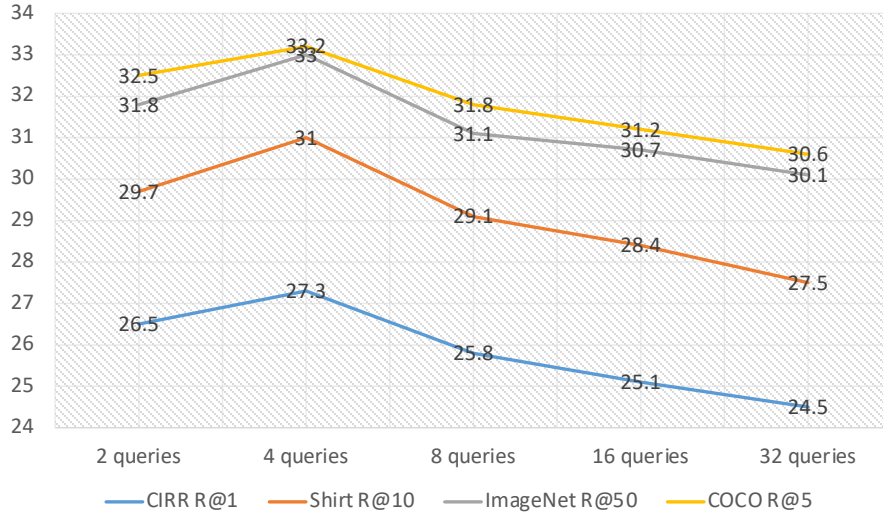


Figure 8: Analysis of the number of learnable queries.

531 when n is added to 32, it is redundant and unhelpful for the CLIP model to understand manipulation
 532 intentions. We finally choose $n = 4$, which gives the best result among different settings.

Table 6: Results on ImageNet for domain conversion.

Methods	Conferences	Cartoon		Origami		Toy		Sculpture		Average	
		R10	R50	R10	R50	R10	R50	R10	R50	R10	R50
Pic2Word [45]	CVPR 2023	8.0	21.9	13.5	25.6	8.7	21.6	10.0	23.8	10.1	23.2
Context-I2W [52]	AAAI 2024	10.2	26.1	17.5	28.7	11.6	27.4	12.1	28.2	12.9	27.6
Context-I2W*	–	11.2	27.4	18.7	30.4	12.5	29.8	13.7	31.4	14.0	29.8
Context-I2W(50%)	AAAI 2024	9.0	23.0	14.3	25.6	10.7	25.0	11.0	25.5	11.3	24.8
De-MINDS(50%)	–	11.7	28.3	19.2	30.9	12.8	30.2	14.2	32.0	14.5	30.4
De-MINDS(100%)	–	13.3	31.2	20.3	34.5	14.7	31.7	16.5	34.7	16.2	33.0

Table 7: Results on CIRR for object manipulation task.

Methods	R1	R5	R10	R50
Pic2Word [45]	23.9	51.7	65.3	87.8
CIReVL [25]	24.6	52.3	64.9	86.3
LinCIR [20]	25.0	53.3	66.7	–
SEARLE-XL [3]	24.2	52.4	66.3	88.6
SEARLE-XL*	25.4	54.1	66.9	89.3
Context-I2W [52]	25.6	55.1	68.5	89.8
Context-I2W*	26.3	55.7	69.0	90.2
Context-I2W(50%)	24.8	53.6	67.1	88.9
De-MINDS (50%)	26.5	56.0	69.3	90.5
De-MINDS	27.3	57.0	71.3	91.6

Table 8: Results on COCO for object composition task.

Methods	R1	R5	R10
Pic2Word [45]	11.5	24.8	33.4
Context-I2W [52]	13.5	28.5	38.1
Context-I2W*	14.3	29.7	40.5
Context-I2W(50%)	12.1	25.6	34.4
De-MINDS (50%)	14.6	30.4	40.8
De-MINDS (100%)	15.7	33.2	44.1

533 A.2 More Effectiveness and Efficiency Analysis

534 In Table 6 to 9, we present more evidence supporting the efficacy and efficiency of our De-MINDS.
 535 With only 50% of the training data, De-MINDS matches and exceeds the performance of the state-
 536 of-the-art (SoTA) Context-I2W model by 0.83% to 2.20%. Remarkably, De-MINDS outperforms
 537 reported results of the SoTA model by 1.98% to 4.57% under the same 50% training data, underscoring
 538 our method’s superiority.

Table 9: Results on Fashion-IQ for attribute manipulation.

Methods	Conferences	Dress		Shrit		TopTee		Average	
		R10	R50	R10	R50	R10	R50	R10	R50
Pic2Word [45]	CVPR 2023	20.0	40.2	26.2	43.6	27.9	47.4	24.7	43.7
CIReVL [25]	ICLR 2024	24.6	44.8	29.5	47.4	31.4	53.7	28.6	48.6
LinCIR [20]	CVPR 2024	20.9	42.4	29.1	46.8	28.8	50.2	26.3	46.5
SEARLE-XL [3]	ICCV 2023	20.3	43.2	27.4	45.7	29.3	50.2	25.7	46.3
SEARLE-XL*	-	22.7	45.0	29.4	47.9	30.2	51.4	27.4	48.1
Context-I2W [52]	AAAI 2024	23.1	45.3	29.7	48.6	30.6	52.9	27.8	48.9
Context-I2W*	-	23.9	46.9	30.4	49.7	31.1	53.8	28.5	50.1
Context-I2W(50%)	AAAI 2024	21.4	43.7	28.1	46.9	29.7	51.4	26.4	47.3
De-MINDS (50%)	-	24.3	47.5	30.6	50.0	31.3	54.0	28.7	50.5
De-MINDS (100%)	-	25.2	48.7	31.0	51.2	32.9	55.7	29.7	51.9

Algorithm 1 Manipulation Intention Understanding’s process.

Input: batch of word embeddings of target descriptions $\tilde{T} = \{\mathbf{t}_i\}_{i=1}^m$, where \mathbf{t}_1 is the global feature \mathbf{t}_{cls} , N_{layer} , the frozen CLIP language encoder Ψ_T

Parameter: a set of learnable embeddings $\mathbf{X} \in \mathbb{R}^{d \times n}$, 8-heads attention layer $Attn$, 3-layers FC layers f_M , $gate_\alpha$.

Output: target embedding $\hat{\mathbf{t}}$

- 1: Initialize $\mathbf{X} \in \mathbb{R}^{d \times n}$, $Attn$, f_M randomly.
- 2: Let $\mathbf{X}_{att}^i = \{\mathbf{t}_i\}_{i=2}^m$, $t = 1$
- 3: **while** $t \leq N_{layer}$ **do**
- 4: $\mathbf{X}_{att}^{i+1} = \mathbf{X}_{att}^i + Attn_t(q=\mathbf{q}, k=concat([\mathbf{X}_{att}^i, \mathbf{q}]), v=concat([\mathbf{X}_{att}^i, \mathbf{q}]))$
- 5: $\mathbf{X}_{att}^{i+1} = \mathbf{X}_{att}^{i+1} + f_{M_t}(\mathbf{X}_{att}^{i+1})$
- 6: $t = t + 1$
- 7: **end while**
- $\mathbf{t}_* = \Psi_T(\mathbf{X}_{output})$
- $\hat{\mathbf{t}} = \mathbf{t}_{cls} + tanh(gate_\alpha) \cdot \mathbf{t}_*$
- 8: **return** $\hat{\mathbf{t}}$

539 **A.3 Broader Impact**

540 We propose a novel image-text dataset augmentation strategy that generates diverse rewrites for
541 any given image-text pair. This approach not only bolsters the performance of vision-language
542 models but also enhances capabilities in textual inversion [44], including text-to-image generation
543 via diffusion models and personalized image retrieval. However, it is crucial to note that MLLMs are
544 trained on extensive web data, which may incorporate factual inaccuracies and hallucinatory content.
545 Consequently, the intention-infused versions of texts could inherit these flaws. We advocate for
546 the implementation of rigorous data filtering methods before these models’ deployment in practical
547 settings. Furthermore, while the MLLM-based rewriting strategy demands substantial GPU/TPU
548 computational resources, potentially increasing the carbon footprint.

549 **A.4 Qualitative Results of intent-CC3M**

550 Figure 9 to 10 we leverage DALL-E [42] to generate images of each caption for qualitative experiment.
551 We compare intent-CC3M with the CC3M dataset and GPT4’s rewritten captions. We found that
552 the captions of Intent-CC3M, which contain potential manipulation intentions, provide better visual
553 information compared to the original captions and those rewritten by a large language model. This
554 improvement is due to incorporating diverse visual perspectives (e.g., colors, scenes, and objects)
555 using a multi-model language model, which enhances the training of text-to-image generation tasks.
556 Notably, our pseudo-manipulation descriptions are shorter than the rewritten captions. The results
557 show that pseudo-manipulation descriptions serve as more effective prompts, enabling DALL-E to
558 generate results that are closer to the original images. This demonstrates the high quality of our
559 pseudo-manipulation descriptions.











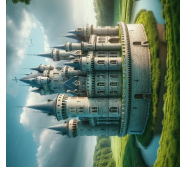



Original Caption	Original Image	LLM's Rewritten Caption	Generated Image	Our Rewritten Caption	Generated Image	Pseudo-Manipulation Generated Image	Description
a street musician plays an accordion.		A street performer serenades passersby with the melodies of an accordion.		A man is playing an accordion on a street. He is standing in the foreground, holding the accordion in his hands. There are several chairs and tables in the background, suggesting a cafe or outdoor seating area. The man is smiling, indicating he is enjoying his performance. The accordion is black and has a metallic finish. The street is lined with buildings, and there are a few other people in the background.			Man plays accordion joyfully in the street, with cafe background suggesting a lively, public musical performance.
Automotive industry now offers a new tuning package for automobile model.		The automotive industry now introduces a fresh tuning package for a specific car model.		A black Volkswagen Beetle is in motion on a road. The car is equipped with a new tuning package, featuring a body kit with a front bumper, side skirts, and a rear bumper, all in the same black color. The car's sleek and modern design has a glossy finish that reflects the surrounding environment. The background is a blur of greenery, which contrasts with the car's urban aesthetic. The domain of the image is photography, capturing a real-life scene.			Highlights Black VW Beetle with tuning package, sleek design, and glossy finish, emphasizing driving on rural road.
on a sunny winter day.		Underneath the crisp winter sun.		A large, round, stone castle with multiple towers stands in the middle of a lush green field. The castle is surrounded by a moat, and the sky is clear and blue. The sun is shining brightly, casting long shadows and highlighting the textures of the stone. The castle is the central focus of the image, with the open field stretching out around it.			A large, round, stone castle with multiple towers, highlighted by stands in the middle of a lush green field, surrounded by a moat, under a clear blue sky.
I start the season with a big tree.		I kick off the season with a towering tree.		A large, leafy tree stands prominently in the center of a town square, surrounded by white buildings with blue accents. The tree is the focal point, with its vibrant green leaves contrasting against the clear blue sky. The town square is bustling with people, adding life to the scene. The architecture of the buildings suggests a European influence, and the overall atmosphere is serene and picturesque.			A large tree in the center of a town square, surrounded by white buildings with blue accents, under a blue sky. The square is bustling with people, showcasing a European-influenced architecture.

Figure 9: Qualitative results of our intent-CC3M dataset. We leverage DALL-E to generate images of the captions. We compare intent-CC3M with the CC3M dataset and LLM’s rewritten captions.

Original Caption	Original Image	LLM's Rewritten Caption	Generated Image	Our Rewritten Caption	Generated Image	Pseudo-Manipulation Generated Image	Description
A toddler laughs in enjoyment on the playground.		A young child giggles with delight while playing on the playground.		A young girl is sitting on a playground swing, laughing and enjoying herself. She is wearing a colorful dress and has blonde hair. Two adults are standing nearby, watching her with smiles. The swing is yellow and has a wooden seat. In the background, there is a sandy area and a fence. The scene is set in a park-like environment.			A young girl is laughing on a swing, wearing a colorful dress, with two adults watching her. The swing is yellow and wooden. They are in a park-like setting.
a shepherd pictured with his flock of sheep in north.		A shepherd captured alongside his flock of sheep in the northern region.		A man in a plaid shirt and a flat cap stands in a field with a flock of sheep. He is smiling and looking directly at the camera. The sheep are scattered around him, grazing on the grass. The sky is clear and blue, suggesting a sunny day. The man's attire and the presence of the sheep suggest a rural or pastoral setting. The image captures a moment of peaceful coexistence between the man and his flock.			Man in plaid shirt and flat cap stands in field with sheep, smiling, looking at camera, on clear, blue day.
A child touches an ice sculpture.		A child reaches out to touch an ice sculpture.		A child reaches out to touch a large ice sculpture of a dragon, which is intricately designed with scales and spikes. The sculpture is positioned on a sandy ground, and the child is standing in front of it. The background is dark, highlighting the brightness of the ice sculpture. The dragon sculpture is made of ice and is the main focus of the image. The child's interaction with the sculpture suggests a sense of wonder and curiosity.			Child reaches out to touch ice dragon sculpture, intricately designed with scales and spikes, standing in front of it on sandy ground.
office worker sitting at the table and working on the computer .		An office worker sits at their desk, diligently working on their computer.		A man is seated at a desk, engrossed in work on his computer. The desk is equipped with a monitor, keyboard, and mouse. The man is dressed in a casual outfit, wearing glasses and has a slight smile on his face. The background is minimalist with a light beige color, and there's a window that lets in natural light. The overall style of the image is a flat illustration with a limited color palette, giving it a modern and clean look.			A man works on his computer at a desk with a monitor, keyboard, and mouse. He is dressed casually, wearing glasses, and has a slight smile. The background is minimalist. The style is a flat illustration with a limited color palette.

Figure 10: Qualitative results of our intent-CC3M dataset. We leverage DALL-E to generate images of the captions. We compare intent-CC3M with the CC3M dataset and LLM's rewritten captions.

560 **B Algorithm of Manipulation Intention Understanding’s Process.**

561 Algorithm 1 outlines the pseudo-code for the manipulation intention understanding process. We
 562 create a fixed number of learnable embeddings as latent queries to capture intentions that the user
 563 aims to modify within manipulation descriptions. These learnable embeddings are then employed in
 564 a Transformer to execute cross-attention with the target descriptions word embedding $\{t_i\}_{i=2}^m$. The
 565 number of output tokens produced by the De-MINDS matches the count of learnable embeddings. To
 566 enhance the interaction between learnable embeddings and word embeddings, we concatenate the
 567 learnable embeddings with keys and values during the cross-attention process. Each learned query
 568 interacts with different intentions, as shown in Figure 2. To achieve a dynamic ratio during the fusion
 569 of global and intention embeddings, we utilize a tanh-gating mechanism [23].

Table 10: More ablation study on CIRR and FashionIQ.

Methods	CIRR			Fashion-IQ	
	R1	R5	R10	R10	R50
1. 100% original caption	26.2	55.5	69.5	26.8	49.9
2. 100% rewritten caption	25.8	55.4	69.0	26.5	49.6
3. 100% pseudo-manipulation description	25.3	54.5	68.0	26.9	49.7
4. 50% original, 50% rewritten	26.5	55.9	70.3	27.7	50.9
5. 50% original, 50% pseudo	25.5	55.2	68.6	27.0	50.1
6. 50% rewritten, 50% pseudo	25.9	55.8	69.7	27.4	50.5
7. 40% original , 30% rewritten , 30% pseudo	26.1	55.7	69.2	28.1	50.1
8. 50% original , 25% rewritten , 25% pseudo	26.7	56.5	70.4	29.2	51.4
9. 50% original , 30% rewritten , 20% pseudo	27.3	57.0	71.3	29.7	51.9
10. w/o align loss	20.6	45.2	57.3	23.6	42.8

570 **C Further Ablation Studies on the Training Strategy**

571 Table 10 details additional ablation analyses of the training strategy in De-MINDS. **In model**
 572 **‘1-10’, we evaluate the necessity of constructs T for pre-training** Our method supports two
 573 scenarios in manipulation intention understanding: integrating intention information from lengthy
 574 texts and deducing it from concise texts. We evaluated the utility of the original caption T_{rew} , the
 575 rewritten caption T_{ori} , and the pseudo-manipulation description T_{int} in fostering an understanding of
 576 manipulation intentions and ensuring training stability. Our experiments led to the optimal ratio of
 577 50% original caption, 30% rewritten caption, and 20% pseudo-manipulation description. Moreover,
 578 **in model ‘9-10’, we assess the significance of the alignment loss.** The absence of alignment
 579 between the original image embedding and the target embedding in pre-training results in a notable
 580 decrease in average performance by 9.54%. This highlights the crucial role of aligning the original
 581 image during training, as in CIR, both the reference image and the manipulation intention together
 582 create a comprehensive context that defines the target image.

583 **D More Details of De-MINDS**

584 **D.1 More Implementation Details For Baseline Models And Mapping Network**

585 Generating one intention caption through LLaVA-1.6-13B [32] for the entire Conceptual Caption
 586 dataset [47], which comprises 3M images (CC3M) dataset requires approximately 625 hours on 5
 587 A100 GPUs. By leveraging the capabilities of LLaVA, we ensure that each text sample within the
 588 dataset is enriched with diverse and contextually intent-relevant text rewrites, significantly enhancing
 589 the dataset’s utility for composed image retrieval tasks. For training De-MINDS, we utilize the CC3M
 590 and adopt ViT-L/14 CLIP [41] pre-trained on 400M image-text paired data. We employ AdamW [34]
 591 with a learning rate of 1×10^{-6} , weight decay of 0.1, and a linear warmup of 10000 steps. The batch
 592 size for contrastive learning is 1024. To improve training stability, we initialize the learnable scalar of
 593 tanh-gating to 0 [2]. For training Context-I2W, we only replace the original captions of CC3M with
 594 our pseudo-manipulation descriptions. Specifically, we employ AdamW [34] with a learning rate of
 595 1×10^{-5} , weight decay of 0.1, and a linear warmup of 10000 steps. The batch size for contrastive

596 learning is 1024. For training SEARLE, we utilize the ImageNet1K [16] test set, which comprises
 597 100K images, and leverage LLaVA to generate intention captions as detailed in Section 3.2. We
 598 employ AdamW, with a learning rate of 5×10^{-5} and a batch size of 256. All models are trained
 599 on 4 NVIDIA A100 (80G) GPUs. Moreover, we conduct ablation studies on CIRR test sets and
 600 FashionIQ validation sets. For FashionIQ, we consider the average recall. To ensure reliable results,
 601 we report the performance averaged over three trials.

602 **Mapping network design.** Table 11 summarizes the mapping network f_θ architecture we employ.

Table 11: Pytorch-style[40] model description of the mapping network f_θ . The output is fed into the CLIP language encoder.

Layer	Module
Output	nn.Linear(512, 768)
ReLU2	nn.ReLU
Dropout2	nn.Dropout(0.1)
FC2	nn.Linear(512, 512)
ReLU1	nn.ReLU
Dropout1	nn.Dropout(0.1)
FC1	nn.Linear(512, 512)

603 **D.2 More Evaluation Datasets Details of Query and Candidate Images.**

604 We evaluate our model on four ZS-CIR datasets, *i.e.*, COCO [31] for object composition, ImageNet
 605 [16, 21] for domain conversion, CIRR [33] for object/scene manipulation, and Fashion-IQ [57] for
 606 attribute manipulation. All the dataset settings and evaluation metrics (Recall@K) follow the recent
 607 works [45, 52] for a fair comparison. The evaluation datasets are preprocessed, as explained in the
 608 main paper, we describe the details of the dataset, *i.e.*, number of query images and candidate images
 609 used for evaluation.

Table 12: The number of images used for evaluation in each dataset.

Dataset	Query images	Candidate images
ImageNet	10,000	16,983
COCO	4,766	4,766
CIRR (test)	4,148	2,315
Fashion (Dress)	2,017	3,817
Fashion (Shirt)	2,038	6,346
Fashion (TopTee)	1,961	5,373

610 **D.3 More Inference Details of Prompts for Different Evaluate Tasks**

611 **(1) Domain conversion.** This setup evaluates the ability to compose real images and domain infor-
 612 mation to retrieve corresponding domain-specific images. We utilize ImageNet [16] and ImageNet-R
 613 [21], which comprises 200 classes with diverse domains and has domain annotations. Following
 614 Pic2Word, we pick cartoon, origami, toy, and sculpture as the evaluation target to avoid noise in the
 615 annotations. With this selection, we have 16,983 images as candidates. In the evaluation, given the
 616 real image from ImageNet and target domain names, we compose the query following the procedure
 617 in (a) in the Inference section. *e.g.*, a cartoon of [*].

618 **(2) Object composition.** We evaluate the validation split (5000 images) of COCO [31], which
 619 dataset contains images with corresponding lists of object classes and instance mask of query images.
 620 Following Pic2Word, we randomly crop one object and mask its background using its instance mask
 621 to create a query for each image. The list of object classes is used as text specification. Given the
 622 reference image and class list, we compose a query by following (b) in the Inference section. *e.g.*, a
 623 photo of [*], [cat] and [dog].

624 **(3) Object/scene manipulation by text description.** In this setup, a reference image is provided
 625 alongside a text description containing instructions for manipulating either an object or the background

626 scene depicted in the reference image. This composition of the reference image and text description
627 enables the retrieval of manipulated images. We evaluate the test split of CIRR [33] using the standard
628 evaluation protocol following previous works [45, 3, 52], and query texts are composed following the
629 procedure in (c) of the Inference section.

630 **(4) Attribute manipulation.** We employ Fashion-IQ [57], which includes various modification texts
631 related to image attributes. These attribute manipulations are given as a sentence. As with CIRR, we
632 adopt the standard evaluation protocol and create query texts following the procedure provided in
633 (c) of the Inference section. In evaluation, we employ the validation set, following previous works
634 [4, 45, 3, 52].

635 E Extended Related Works

636 **Mapping Image as One Word.** Several methods [30, 59] represent image regions as word tokens via
637 VLP models, which rely on object detector efficacy. However, ZR-CIR tasks extend the alignment
638 ability beyond objects to scenes, styles, attributes, *ect*. Our method addresses this issue by employing
639 pseudo triplet data, which maps a pseudo reference image to a pseudo word token and combines it
640 with the caption to align with the target image. PALAVRA [14] proposes personalized image retrieval
641 via cycle contrastive loss, requiring class-wise and caption annotations. In contrast, our model
642 facilitates fine-grained image-to-word mapping without additional annotations. Other approaches
643 [26, 36, 62, 50] utilize a single word token to represent multiple images of the same object for
644 text-to-image generation. Our model obviates the need for costly image-supervised training.

645 **Knowledge Distillation.** Knowledge distillation is a machine learning technique wherein a simpler
646 model, known as the student, learns to mimic the behavior of a more complex model, known as
647 the teacher, by learning from its predictions [22]. This approach has demonstrated efficacy across
648 various computer vision tasks, including image classification [22, 43, 5], object detection [9, 8],
649 and text-to-image synthesis [35, 46], resulting in improved model compression, computational
650 efficiency, and accuracy. In our study, we employ knowledge distillation to transfer knowledge from
651 a computationally expensive optimization method (teacher) to a more lightweight neural network
652 (student). Specifically, we train a manipulation intention understanding network to replicate the
653 reasoning ability of an MLLM using a distillation loss. Alternatively, our lightweight network can be
654 interpreted as a surrogate model of the more resource-intensive technique.

655 **NeurIPS Paper Checklist**

656 **1. Claims**

657 Question: Do the main claims made in the abstract and introduction accurately reflect the
658 paper's contributions and scope?

659 Answer: [Yes]

660 Justification: The abstract and introduction are include the claims made in the paper

661 Guidelines:

- 662 • The answer NA means that the abstract and introduction do not include the claims
663 made in the paper.
- 664 • The abstract and/or introduction should clearly state the claims made, including the
665 contributions made in the paper and important assumptions and limitations. A No or
666 NA answer to this question will not be perceived well by the reviewers.
- 667 • The claims made should match theoretical and experimental results, and reflect how
668 much the results can be expected to generalize to other settings.
- 669 • It is fine to include aspirational goals as motivation as long as it is clear that these goals
670 are not attained by the paper.

671 **2. Limitations**

672 Question: Does the paper discuss the limitations of the work performed by the authors?

673 Answer: [Yes]

674 Justification: Our paper has limitation in our main paper.

675 Guidelines:

- 676 • The answer NA means that the paper has no limitation while the answer No means that
677 the paper has limitations, but those are not discussed in the paper.
- 678 • The authors are encouraged to create a separate "Limitations" section in their paper.
- 679 • The paper should point out any strong assumptions and how robust the results are to
680 violations of these assumptions (e.g., independence assumptions, noiseless settings,
681 model well-specification, asymptotic approximations only holding locally). The authors
682 should reflect on how these assumptions might be violated in practice and what the
683 implications would be.
- 684 • The authors should reflect on the scope of the claims made, e.g., if the approach was
685 only tested on a few datasets or with a few runs. In general, empirical results often
686 depend on implicit assumptions, which should be articulated.
- 687 • The authors should reflect on the factors that influence the performance of the approach.
688 For example, a facial recognition algorithm may perform poorly when image resolution
689 is low or images are taken in low lighting. Or a speech-to-text system might not be
690 used reliably to provide closed captions for online lectures because it fails to handle
691 technical jargon.
- 692 • The authors should discuss the computational efficiency of the proposed algorithms
693 and how they scale with dataset size.
- 694 • If applicable, the authors should discuss possible limitations of their approach to
695 address problems of privacy and fairness.
- 696 • While the authors might fear that complete honesty about limitations might be used by
697 reviewers as grounds for rejection, a worse outcome might be that reviewers discover
698 limitations that aren't acknowledged in the paper. The authors should use their best
699 judgment and recognize that individual actions in favor of transparency play an impor-
700 tant role in developing norms that preserve the integrity of the community. Reviewers
701 will be specifically instructed to not penalize honesty concerning limitations.

702 **3. Theory Assumptions and Proofs**

703 Question: For each theoretical result, does the paper provide the full set of assumptions and
704 a complete (and correct) proof?

705 Answer: [Yes]

706 Justification: All the formulas in the paper be numbered and cross-referenced

707 Guidelines:

- 708 • The answer NA means that the paper does not include theoretical results.
- 709 • All the theorems, formulas, and proofs in the paper should be numbered and cross-
- 710 referenced.
- 711 • All assumptions should be clearly stated or referenced in the statement of any theorems.
- 712 • The proofs can either appear in the main paper or the supplemental material, but if
- 713 they appear in the supplemental material, the authors are encouraged to provide a short
- 714 proof sketch to provide intuition.
- 715 • Inversely, any informal proof provided in the core of the paper should be complemented
- 716 by formal proofs provided in appendix or supplemental material.
- 717 • Theorems and Lemmas that the proof relies upon should be properly referenced.

718 4. Experimental Result Reproducibility

719 Question: Does the paper fully disclose all the information needed to reproduce the main ex-

720 perimental results of the paper to the extent that it affects the main claims and/or conclusions

721 of the paper (regardless of whether the code and data are provided or not)?

722 Answer: [Yes]

723 Justification: The code and sample dataset are provided in our supplementary. We describe

724 the steps taken to make the results reproducible or verifiable.

725 Guidelines:

- 726 • The answer NA means that the paper does not include experiments.
- 727 • If the paper includes experiments, a No answer to this question will not be perceived
- 728 well by the reviewers: Making the paper reproducible is important, regardless of
- 729 whether the code and data are provided or not.
- 730 • If the contribution is a dataset and/or model, the authors should describe the steps taken
- 731 to make their results reproducible or verifiable.
- 732 • Depending on the contribution, reproducibility can be accomplished in various ways.
- 733 For example, if the contribution is a novel architecture, describing the architecture fully
- 734 might suffice, or if the contribution is a specific model and empirical evaluation, it may
- 735 be necessary to either make it possible for others to replicate the model with the same
- 736 dataset, or provide access to the model. In general, releasing code and data is often
- 737 one good way to accomplish this, but reproducibility can also be provided via detailed
- 738 instructions for how to replicate the results, access to a hosted model (e.g., in the case
- 739 of a large language model), releasing of a model checkpoint, or other means that are
- 740 appropriate to the research performed.
- 741 • While NeurIPS does not require releasing code, the conference does require all submis-
- 742 sions to provide some reasonable avenue for reproducibility, which may depend on the
- 743 nature of the contribution. For example
- 744 (a) If the contribution is primarily a new algorithm, the paper should make it clear how
- 745 to reproduce that algorithm.
- 746 (b) If the contribution is primarily a new model architecture, the paper should describe
- 747 the architecture clearly and fully.
- 748 (c) If the contribution is a new model (e.g., a large language model), then there should
- 749 either be a way to access this model for reproducing the results or a way to reproduce
- 750 the model (e.g., with an open-source dataset or instructions for how to construct
- 751 the dataset).
- 752 (d) We recognize that reproducibility may be tricky in some cases, in which case
- 753 authors are welcome to describe the particular way they provide for reproducibility.
- 754 In the case of closed-source models, it may be that access to the model is limited in
- 755 some way (e.g., to registered users), but it should be possible for other researchers
- 756 to have some path to reproducing or verifying the results.

757 5. Open access to data and code

758 Question: Does the paper provide open access to the data and code, with sufficient instruc-

759 tions to faithfully reproduce the main experimental results, as described in supplemental

760 material?

761
762
763
764
765
766
767
768
769
770
771
772
773
774
775
776
777
778
779
780
781
782
783
784
785
786
787
788
789
790
791
792
793
794
795
796
797
798
799
800
801
802
803
804
805
806
807
808
809
810
811

Answer: [Yes]

Justification: Our paper provides open access to the code for creating the dataset and reproducing the main experimental results. We will provide the entire dataset after our paper is accepted.

Guidelines:

- The answer NA means that paper does not include experiments requiring code.
- Please see the NeurIPS code and data submission guidelines (<https://nips.cc/public/guides/CodeSubmissionPolicy>) for more details.
- While we encourage the release of code and data, we understand that this might not be possible, so “No” is an acceptable answer. Papers cannot be rejected simply for not including code, unless this is central to the contribution (e.g., for a new open-source benchmark).
- The instructions should contain the exact command and environment needed to run to reproduce the results. See the NeurIPS code and data submission guidelines (<https://nips.cc/public/guides/CodeSubmissionPolicy>) for more details.
- The authors should provide instructions on data access and preparation, including how to access the raw data, preprocessed data, intermediate data, and generated data, etc.
- The authors should provide scripts to reproduce all experimental results for the new proposed method and baselines. If only a subset of experiments are reproducible, they should state which ones are omitted from the script and why.
- At submission time, to preserve anonymity, the authors should release anonymized versions (if applicable).
- Providing as much information as possible in supplemental material (appended to the paper) is recommended, but including URLs to data and code is permitted.

6. Experimental Setting/Details

Question: Does the paper specify all the training and test details (e.g., data splits, hyper-parameters, how they were chosen, type of optimizer, etc.) necessary to understand the results?

Answer: [Yes]

Justification: Our paper specifies all the training and test details in the main paper and appendix. We also provide the pseudo-code for our method in our appendix.

Guidelines:

- The answer NA means that the paper does not include experiments.
- The experimental setting should be presented in the core of the paper to a level of detail that is necessary to appreciate the results and make sense of them.
- The full details can be provided either with the code, in appendix, or as supplemental material.

7. Experiment Statistical Significance

Question: Does the paper report error bars suitably and correctly defined or other appropriate information about the statistical significance of the experiments?

Answer: [No]

Justification: Error bars are not reported because it would be too computationally expensive for four datasets.

Guidelines:

- The answer NA means that the paper does not include experiments.
- The authors should answer "Yes" if the results are accompanied by error bars, confidence intervals, or statistical significance tests, at least for the experiments that support the main claims of the paper.
- The factors of variability that the error bars are capturing should be clearly stated (for example, train/test split, initialization, random drawing of some parameter, or overall run with given experimental conditions).

- 812 • The method for calculating the error bars should be explained (closed form formula,
813 call to a library function, bootstrap, etc.)
- 814 • The assumptions made should be given (e.g., Normally distributed errors).
- 815 • It should be clear whether the error bar is the standard deviation or the standard error
816 of the mean.
- 817 • It is OK to report 1-sigma error bars, but one should state it. The authors should
818 preferably report a 2-sigma error bar than state that they have a 96% CI, if the hypothesis
819 of Normality of errors is not verified.
- 820 • For asymmetric distributions, the authors should be careful not to show in tables or
821 figures symmetric error bars that would yield results that are out of range (e.g. negative
822 error rates).
- 823 • If error bars are reported in tables or plots, The authors should explain in the text how
824 they were calculated and reference the corresponding figures or tables in the text.

8. Experiments Compute Resources

826 Question: For each experiment, does the paper provide sufficient information on the com-
827 puter resources (type of compute workers, memory, time of execution) needed to reproduce
828 the experiments?

829 Answer: [Yes]

830 Justification: We indicate the type of compute workers and compute time for dataset
831 generation and training.

832 Guidelines:

- 833 • The answer NA means that the paper does not include experiments.
- 834 • The paper should indicate the type of compute workers CPU or GPU, internal cluster,
835 or cloud provider, including relevant memory and storage.
- 836 • The paper should provide the amount of compute required for each of the individual
837 experimental runs as well as estimate the total compute.
- 838 • The paper should disclose whether the full research project required more compute
839 than the experiments reported in the paper (e.g., preliminary or failed experiments that
840 didn't make it into the paper).

841 9. Code Of Ethics

842 Question: Does the research conducted in the paper conform, in every respect, with the
843 NeurIPS Code of Ethics <https://neurips.cc/public/EthicsGuidelines?>

844 Answer: [Yes]

845 Justification: We have reviewed the NeurIPS Code of Ethics.

846 Guidelines:

- 847 • The answer NA means that the authors have not reviewed the NeurIPS Code of Ethics.
- 848 • If the authors answer No, they should explain the special circumstances that require a
849 deviation from the Code of Ethics.
- 850 • The authors should make sure to preserve anonymity (e.g., if there is a special consid-
851 eration due to laws or regulations in their jurisdiction).

852 10. Broader Impacts

853 Question: Does the paper discuss both potential positive societal impacts and negative
854 societal impacts of the work performed?

855 Answer: [Yes]

856 Justification: We discuss both potential positive societal impacts and negative societal
857 impacts of the work performed in our appendix.

858 Guidelines:

- 859 • The answer NA means that there is no societal impact of the work performed.
- 860 • If the authors answer NA or No, they should explain why their work has no societal
861 impact or why the paper does not address societal impact.

- 862
- 863
- 864
- 865
- 866
- 867
- 868
- 869
- 870
- 871
- 872
- 873
- 874
- 875
- 876
- 877
- 878
- 879
- 880
- Examples of negative societal impacts include potential malicious or unintended uses (e.g., disinformation, generating fake profiles, surveillance), fairness considerations (e.g., deployment of technologies that could make decisions that unfairly impact specific groups), privacy considerations, and security considerations.
 - The conference expects that many papers will be foundational research and not tied to particular applications, let alone deployments. However, if there is a direct path to any negative applications, the authors should point it out. For example, it is legitimate to point out that an improvement in the quality of generative models could be used to generate deepfakes for disinformation. On the other hand, it is not needed to point out that a generic algorithm for optimizing neural networks could enable people to train models that generate Deepfakes faster.
 - The authors should consider possible harms that could arise when the technology is being used as intended and functioning correctly, harms that could arise when the technology is being used as intended but gives incorrect results, and harms following from (intentional or unintentional) misuse of the technology.
 - If there are negative societal impacts, the authors could also discuss possible mitigation strategies (e.g., gated release of models, providing defenses in addition to attacks, mechanisms for monitoring misuse, mechanisms to monitor how a system learns from feedback over time, improving the efficiency and accessibility of ML).

881 11. Safeguards

882 Question: Does the paper describe safeguards that have been put in place for responsible
883 release of data or models that have a high risk for misuse (e.g., pretrained language models,
884 image generators, or scraped datasets)?

885 Answer: [No]

886 Justification: our paper poses no such risks.

887 Guidelines:

- 888
- 889
- 890
- 891
- 892
- 893
- 894
- 895
- 896
- 897
- The answer NA means that the paper poses no such risks.
 - Released models that have a high risk for misuse or dual-use should be released with necessary safeguards to allow for controlled use of the model, for example by requiring that users adhere to usage guidelines or restrictions to access the model or implementing safety filters.
 - Datasets that have been scraped from the Internet could pose safety risks. The authors should describe how they avoided releasing unsafe images.
 - We recognize that providing effective safeguards is challenging, and many papers do not require this, but we encourage authors to take this into account and make a best faith effort.

898 12. Licenses for existing assets

899 Question: Are the creators or original owners of assets (e.g., code, data, models), used in
900 the paper, properly credited and are the license and terms of use explicitly mentioned and
901 properly respected?

902 Answer: [Yes]

903 Justification: the creators or original owners of assets are the license and terms of use
904 explicitly mentioned and properly respected.

905 Guidelines:

- 906
- 907
- 908
- 909
- 910
- 911
- 912
- The answer NA means that the paper does not use existing assets.
 - The authors should cite the original paper that produced the code package or dataset.
 - The authors should state which version of the asset is used and, if possible, include a URL.
 - The name of the license (e.g., CC-BY 4.0) should be included for each asset.
 - For scraped data from a particular source (e.g., website), the copyright and terms of service of that source should be provided.

- 913
- 914
- 915
- 916
- 917
- 918
- 919
- 920
- If assets are released, the license, copyright information, and terms of use in the package should be provided. For popular datasets, paperswithcode.com/datasets has curated licenses for some datasets. Their licensing guide can help determine the license of a dataset.
 - For existing datasets that are re-packaged, both the original license and the license of the derived asset (if it has changed) should be provided.
 - If this information is not available online, the authors are encouraged to reach out to the asset's creators.

921 13. **New Assets**

922 Question: Are new assets introduced in the paper well documented and is the documentation
923 provided alongside the assets?

924 Answer: [No]

925 Justification: Our paper does not release new assets.

926 Guidelines:

- 927
- 928
- 929
- 930
- 931
- 932
- 933
- 934
- The answer NA means that the paper does not release new assets.
 - Researchers should communicate the details of the dataset/code/model as part of their submissions via structured templates. This includes details about training, license, limitations, etc.
 - The paper should discuss whether and how consent was obtained from people whose asset is used.
 - At submission time, remember to anonymize your assets (if applicable). You can either create an anonymized URL or include an anonymized zip file.

935 14. **Crowdsourcing and Research with Human Subjects**

936 Question: For crowdsourcing experiments and research with human subjects, does the paper
937 include the full text of instructions given to participants and screenshots, if applicable, as
938 well as details about compensation (if any)?

939 Answer: [No]

940 Justification: Our paper does not involve crowdsourcing nor research with human subjects.

941 Guidelines:

- 942
- 943
- 944
- 945
- 946
- 947
- 948
- 949
- The answer NA means that the paper does not involve crowdsourcing nor research with human subjects.
 - Including this information in the supplemental material is fine, but if the main contribution of the paper involves human subjects, then as much detail as possible should be included in the main paper.
 - According to the NeurIPS Code of Ethics, workers involved in data collection, curation, or other labor should be paid at least the minimum wage in the country of the data collector.

950 15. **Institutional Review Board (IRB) Approvals or Equivalent for Research with Human 951 Subjects**

952 Question: Does the paper describe potential risks incurred by study participants, whether
953 such risks were disclosed to the subjects, and whether Institutional Review Board (IRB)
954 approvals (or an equivalent approval/review based on the requirements of your country or
955 institution) were obtained?

956 Answer: [No]

957 Justification: Our paper does not involve crowdsourcing nor research with human subjects

958 Guidelines:

- 959
- 960
- 961
- 962
- 963
- The answer NA means that the paper does not involve crowdsourcing nor research with human subjects.
 - Depending on the country in which research is conducted, IRB approval (or equivalent) may be required for any human subjects research. If you obtained IRB approval, you should clearly state this in the paper.

964
965
966
967
968

- We recognize that the procedures for this may vary significantly between institutions and locations, and we expect authors to adhere to the NeurIPS Code of Ethics and the guidelines for their institution.
- For initial submissions, do not include any information that would break anonymity (if applicable), such as the institution conducting the review.